Paleoceanography and Paleoclimatology

RESEARCH ARTICLE
10.1029/2019PA003628

Southern California Vegetation, Wildfire, and Erosion Had Nonlinear Responses to Climatic Forcing During Marine Isotope Stages 5–2 (120–15 ka)

Katherine C. Glover[1,2], April Chaney[2], Matthew E. Kirby[3], William P. Patterson[4], and Glen M. MacDonald[1,5]

[1]Department of Geography, University of California, Los Angeles, CA, USA, [2]Climate Change Institute, University of Maine, Orono, ME, USA, [3]Department of Geological Sciences, California State University, Fullerton, Fullerton, CA, USA, [4]Department of Geological Sciences, University of Saskatchewan, Saskatoon, Saskatchewan, Canada, [5]Institute of the Environment and Sustainability, University of California, Los Angeles, CA, USA

Key Points:
- A multiproxy lake record from montane Southern California showed that summer insolation shifts induced productive lake states periodically from 120 to 15 ka
- Pollen and charcoal variability on $\leq 10^3$ kyr scales suggest hydroclimatic variability as a primary driver of vegetation and wildfire during MIS 4–3
- Steppe expansion occurred during MIS 4, while forest expanded during MIS 2 and responded to regional hydrologic events

Supporting Information:
- Supporting Information S1
- Table S1
- Figure S1
- Figure S2
- Figure S3

Correspondence to:
K. C. Glover,
katherine.glover@maine.edu

Citation:
Glover, K. C., Chaney, A., Kirby, M. E., Patterson, W. P., & MacDonald, G. M. (2020). Southern California vegetation, wildfire, and erosion had nonlinear responses to climatic forcing during marine isotope stages 5–2 (120–15 ka). *Paleoceanography and Paleoclimatology*, *35*, e2019PA003628. https://doi.org/10.1029/2019PA003628

Received 8 APR 2019
Accepted 27 NOV 2019
Accepted article online 23 JAN 2020

Abstract A multiproxy record from Baldwin Lake, San Bernardino Mountains, allowed us to examine variation and relationships between erosion, wildfire, vegetation, and climate in subalpine Southern California from 120 to 15 ka. Bulk organics, biogenic silica, and molar C:N data were generally antiphased with magnetic and trace element data and displayed long-term (10^5 year) shifts between autochthonous and allocthonous deposition. This was most pronounced during Marine Isotope Stage (MIS) 5, and we hypothesize that local summer insolation was the primary driver for Baldwin Lake's productive and unproductive lake state alternations. Wildfire history was inferred from charcoal concentrations and vegetation change from pollen. Relationships between these ecological processes, basin deposition, and summer insolation were often nonlinear. Sagebrush expansion, wildfire, and weak basin weathering characterized MIS 4, while during MIS 2, the basin was highly erosive, rarely burned, and the forest was impacted by shifts in Southern Californian hydroclimate. Despite coniferous forest cover throughout MIS 3, submillennial oscillations in charcoal, pollen, and bulk organic content occurred, consistent with pollen records from Eurasia's Mediterranean biome that span multiple glacial-interglacial cycles. Highly resolved global CO_2 records and sea surface temperatures in key regions of the Pacific show no apparent relationship to these landscape conditions, and we suggest submillennial hydroclimatic variability as a potential driver. Highly resolved long pollen records from Southern California are an urgent research need to better understand the finer-scale ($\leq 10^3$ year) interactions between past vegetation, wildfire, and erosion, given the current natural disaster risks that 21st century climate change poses to both human and ecological communities.

1. Introduction

Mediterranean ecoregions are characterized by a winter-wet summer-dry climate and known for their endemic biota and designation as biodiversity hot spots. Increasingly, climate change and rapid development are threats to these ecosystems (Arianoutsou et al., 2012; Olson et al., 2001; Underwood et al., 2009). California will be especially vulnerable to anticipated climate change (Bedsworth et al., 2018), with temperatures projected to continue increasing for the rest of the 21st century Southern California (IPCC, 2013; Overpeck et al., 2013). Total annual precipitation has increased in since 1901 in the Mediterranean climate region of the North American West Coast (Seager et al., 2019). Both projections for higher temperatures and precipitation will drive evaporative demand that may shift California's Mediterranean biome itself northward (Seager et al., 2019). This could cause antecedent shifts to vegetation zones and the intensity and length of wildfire season (Lenihan et al., 2008). Longer, more intense wildfire seasons have already impacted the North American West since the 1970s (van Mantgem et al., 2009; Westerling, 2006). In the Transverse Ranges of Southern California, the combination of development, drought, tree mortality, and large-scale wildfires has had compounded effects on forest ecosystems (Tullis, 2013; USDA Forest Service, 2005).

We can use lake sediment archives to investigate the natural variability of climate and ecologic processes, their interactions, and climatic responsiveness prior to Euro-American Settlement and instrumental record keeping in Southern California. This yields insight to how the natural environment responded to climate change over long (up to 10^5 year) time scales. In particular, we examine the responsiveness of these

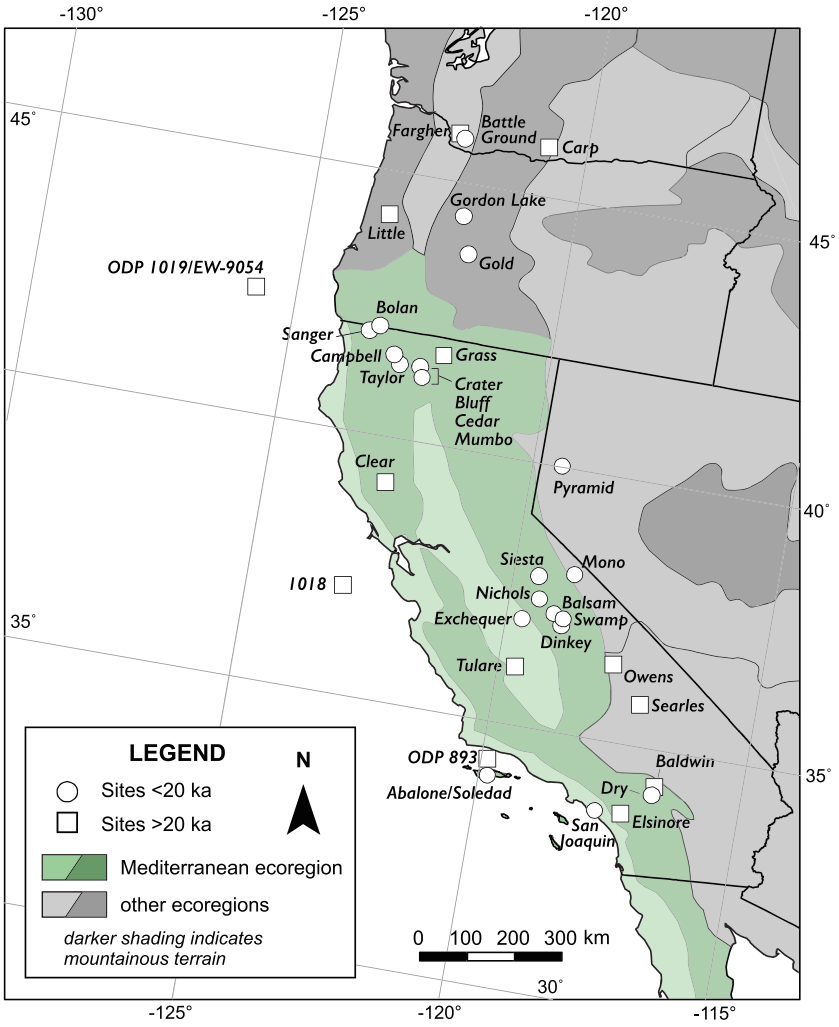

Figure 1. West Coast fossil pollen records that span at least 5 kyr continuously and include one of the following: charcoal, comparison to orbitally-induced insolation, and sedimentary data. Sedimentary data here includes physical properties (e.g., magnetic susceptibility and loss on ignition) and any geochemical proxy. See Table S1 for site details, including age and reference(s).

systems to radiative and oceanic changes related to Milankovitch orbital variations. Whitlock and Grigg (1999) showed that changes in insolation caused by Milankovitch Cycles directly influence vegetation growth on the North American West Coast over multiple Marine Isotope Stages (MISs). Marine records offer an aggregate view of coastal vegetation shifts over time and the influence of the Northern Hemisphere's precessional cycle since 600 ka (ODP 1018, Figure 1; Lyle et al., 2010). Figure 1 shows West Coast paleo sites with pollen records that span at least 5 kyr continuously and have two or more of the following: sedimentary data, charcoal analysis, pollen analysis, and a comparison to orbitally induced radiation. We present here the oldest record for California's Mediterranean subalpine environment with all four of these analyses.

We examined the long-term history (~90 kyr) of erosion, wildfire, and vegetation variability from a ~27 m lake core in the San Bernardino Mountains (SBM). Analyses include fossil pollen, charcoal, trace element, and stable isotopes, and potential climatic influences on the basin and broader Southern California region. Baldwin Lake (2,060 m; Figure 1) is a dry subalpine lake basin on the transition between Mediterranean and Temperate-Subtropical ecoregions. Our record is thus well situated to track landscape response to climate change across MIS 5–2 (120 to 15 ka). We asked the following questions:

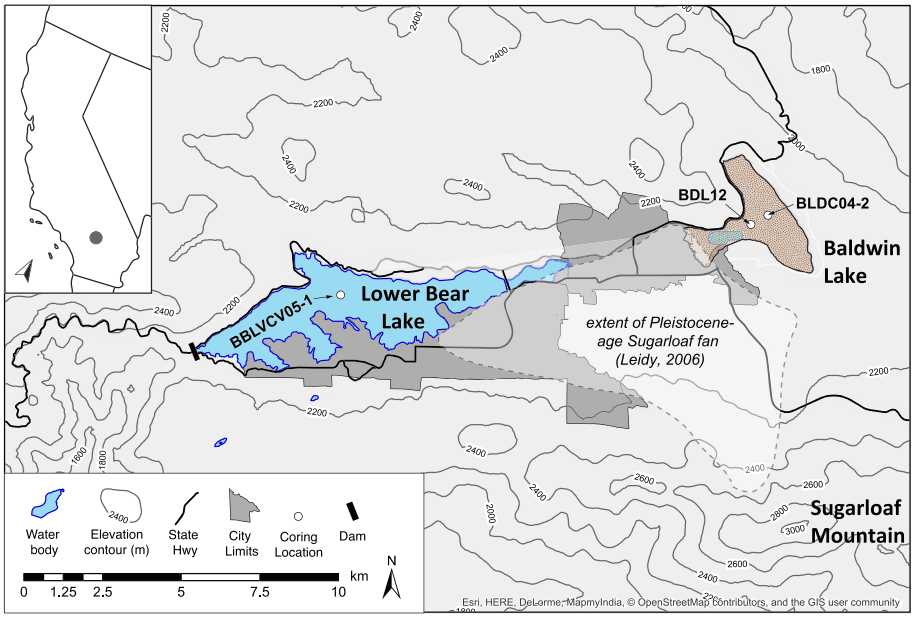

Figure 2. Map of Big Bear Valley lake basins with core locations shown. Core BDL12 was the focus of this work. Reprinted from *Quaternary Science Reviews* 167, Glover, K. C., MacDonald, G. M., Kirby, M. E., Rhodes, E., Stevens, L., Silveira, E., Whittaker, A., and Lydon, S., Evidence for orbital and North Atlantic climate forcing in alpine Southern California between 125 – 10 ka from multi-proxy analyses of Baldwin Lake, 47-62, 2017, with permission from Elsevier.

1. How have erosion, wildfire, and vegetation shifted in Southern California's mountains since 120 ka?
2. Were these phenomena sensitive to insolation forcing?
3. What other potential climatic drivers may have influenced these histories, including those operating on shorter ($\leq 10^3$ year) time scales?

Recent work has shown future scenarios for California and the U.S. Southwest that include climate erraticism (Loisel et al., 2017) and whiplash (Swain et al., 2018). Both of these possibilities come with increased natural disaster risk, including flooding and wildfire. Thus, a better understanding of the natural variability of the Mediterranean biome environment over long time scales is critical.

2. Setting and Background

Baldwin Lake (2,060 m; 34.2761, −116.8100) is an intermittent lake, in a subalpine basin (79 km^2) in Big Bear Valley in the northeastern SBM, part of the Transverse Ranges of Southern California (Figures 1 and 2). Variable terrain, diverse geology, and distinct microclimates create a varied vegetation assemblage (Anderson & Koehler, 2003; Barbour & Billings, 2000; Minnich et al., 1995). This prevailing winter-wet and summer-dry climate produces summer wildfire seasons in the SBM. Local precipitation largely comes from winter Pacific storms and snow drift (Minnich, 1984), and Big Bear Valley has one of the highest annual precipitation totals in Southern California (~220 cm/year; U.S. Climate Data, 2016). Minor amounts from orographic uplift and extratropical storms in the summer supplement this winter-dominated precipitation regime (Tubbs, 1972). A strong precipitation gradient exists along the west-east axis of Big Bear Valley, with an annual precipitation total at its eastern end that averages one third of that from its western end (U.S. Climate Data, 2016).

Valley vegetation cover reflects this precipitation gradient. Pine-dominated coniferous forest typifies the Big Bear Lake basin, a mesic assemblage of *Pinus lambertiana* (sugar pine), *P. jeffreyi* (Jeffrey pine), *P. ponderosa* (Ponderosa pine), *Abies concolor* (white fir), *Calocedrus decurrens* (Incense cedar), and *Quercus kelloggii* (Blue Oak, Anderson & Koehler, 2003). In the Baldwin Lake watershed, vegetation transitions to pinyon-juniper woodland, with relatively xeric taxa that include *Pinus monophylla* (pinyon pine) and *Juniperus occidentalis* (western juniper). This woodland is admixed with Great Basin sagebrush (*Artemisia tridentata*), particularly in the hills, ridges, and higher elevations surrounding Baldwin Lake (Minnich, 1976; Minnich et al.,

1995). Within 1 km of Baldwin Lake's northeastern shoreline, desert taxa occur in this juniper-pinyon-sage woodland. These include *Yucca brevefolia* (Joshua tree), *Ephedra* spp. (Mormon tea), and *Opuntia basilaris* (beavertail cactus; Anderson & Koehler, 2003).

Baldwin Lake thus lies at the transition between Mediterranean woodland and the temperate-subtropical desert that typifies the Mojave Desert (Bailey, 2009). Mediterranean montane vegetation is particularly responsive to long-term shifts in moisture (Jiménez-Moreno et al., 2010) and adapted to wildfire disturbance and the annual cycle of summer drought (Keeley et al., 2012). Other paleorecords in the region have experienced periods of desiccation (e.g., Tulare Lake, Davis, 1999a; Owens Lake, Woolfenden, 2003), as conditions are often drier than sites in northern California and the Pacific Northwest (Figure 1). This creates a scarcity of permanent lakes in Southern California. Conditions in the SBM are an exception, with perennial lake persistence from 120 to 15 kyr. Prior work on Baldwin Lake demonstrated that summer insolation likely influenced its productivity on 10^4 year time scales (Glover et al., 2017) and anoxic conditions resulted in good microfossil preservation. This yielded a record of vegetation response to paleoclimatic change from 108 to 15 ka.

3. Material and Methods

3.1. Core Recovery, Age Model, and Sedimentological Analyses

The Baldwin Lake core (BDL12) is a ~27 m composite sequence of overlapping sections from two adjacent drill holes in Baldwin Lake's depocenter (Figure 2). Coring in 2012 was conducted with a CME-95 truck-mounted hollow stem auger drill and produced a record that was 92% complete. We used Bayesian age-depth modeling program Bacon 2.2 (Blaauw & Christen, 2011) to develop an age model tuned to summer insolation that initially employed 15 radiocarbon dates, luminescence dates, and tie points (Table S2, Glover et al., 2017). We use an untuned version here that was similarly generated in Bacon 2.2, but without tie points. While the untuned model displayed a greater envelope of uncertainty for the time period older than radiocarbon dating limits, we found that weighted mean ages of both models were similar (less than ±2 kyr difference) for 79% of the record, notably from the core top at ~10 ka to 96–98 ka. In both versions, age control in the uppermost 1.5 m in the BDL12 sequence was unreliable, and preservation was poor in these desiccated sediments. Further comparison between the two age models can be found in the supporting information, and we use the untuned version for date estimates in this work.

In our analyses, we define proxy as a qualitative variable used to reconstruct past environmental conditions, in accordance with National Oceanic and Atmospheric Administration usage (NOAA, 2019). Prior proxy analyses on BDL12 targeted its physical, trace element, and biogenic characteristics (Glover et al., 2017). In this work, we aimed to expand our prior focus from largely autochthonous processes toward whole-basin deposition and landscape change. Sedimentological analyses presented here include loss-on-ignition (LOI; Dean, 1974), magnetic susceptibility (Dearing, 1999), grain size analysis, pXRF analysis (Kylander et al., 2011), and biogenic silica (BSi; Conley & Schelske, 2002). Trace element data were measured at 5-cm intervals with a portable XRF Innov-X Analyzer. Titanium (Ti) was examined here as a measure of inorganic basin deposition alongside bulk inorganic deposition, calculated from LOI results.

3.2. Carbon and Nitrogen Analysis

In broadening our scope in this study to include watershed processes, we conducted carbon and nitrogen analysis on select horizons from BDL12. This was low-resolution, exploratory analysis to see if periods of higher molar C/N ratios indicated times of enhanced surface runoff that contributed to greater bulk organic content values. We sampled horizons with variable bulk organic values between 1.9 and 20.3 m depth (~16.0–96.0 ka) to best capture different facies. Samples ($n = 25$) were removed from the split core surface, dried at 60 °C for 24 hr, disaggregated with a mortar and pestle, and weighed. Bulk $CaCO_3$ percentages from LOI analysis were used to determine sample weights that contained at least 20 μg. Total organic nitrogen and carbon were measured at the Saskatchewan Isotope Laboratory after acidification removed carbonate material in a Thermo Finnigan Flash 1112 EA.

3.3. Paleoecological Analyses

3.3.1. Charcoal

Charcoal sampling followed methods outlined in Ballard (2009), with contiguous slices taken from the split core surface that were 4 cm × 1 cm (average time step = 176 years per sample) and cut at an angle to create 2 cm^3 volume. Individual samples were digested in 25 ml 6% H_2O_2 in Erlenmeyer flasks at 50–60 °C. After 72 hr, samples were then sieved through a 125 μm mesh, transferred to individual petri dishes with a few drops of a deflocculant (0.1% sodium hexametaphosphate), and dehydrated at 50 °C (Myrbo et al., 2005). Samples that were too murky to count after the initial treatment were dehydrated in their flask and treated with a second digestion. Macrocharcoal particles (defined here as those ≥125 μm) on the petri dish were counted while overlain on a numbered grid under a binocular microscope at 40–60x magnification. Counts were converted to charcoal accumulation rate (CHAR) values, a measure of the number charcoal particles deposited per cm^2 per year.

3.3.2. Pollen

Samples for pollen were initially taken at 20 cm intervals that spanned 0.8–24 m (8.2–108.2 ka), with some adjustments as the correlation and age model were finalized. Pollen preservation was poor above 14.6 ka and below 103.8 ka, limiting our analysis to ~90 kyr. Portions of MIS 2 (13.6–27.2 ka; 1.7–3.2 m) were later sampled at 10 cm intervals, once its slow sedimentation rate was identified. All 1 cm^3 samples ($n = 89$) underwent standard pollen chemical digestion (Bennett & Willis, 2001; Faegri et al., 1989). Tracer grains of *Lycopodium* were added during initial 10% HCl digestion (Batch 1031, Lund University). Acetolysis was not performed after pilot sample batches, as most grains were identifiable to genus without it.

A minimum of 300 terrestrial pollen grains were identified in each sample. Taxa percentages were calculated using the total terrestrial grains in each sample. Unique taxa with at least one horizon measuring ≥3% were used for CONISS zonation in Tilia 2.0.4.1 software (Grimm, 1987), along with groups of low-concentration taxa (e.g., Taxodiaceae-Cupressaceae-Taxaceae and "Arboreal pollen – other"). Further detail on these aggregate groups is in the supporting information. Pollen accumulation rate (PAR) values were calculated as the product of pollen concentration, estimated using counts of the known-concentration *Lycopodium* spike and the sedimentation rate from the age depth model.

4. Results

4.1. Core Recovery, Sedimentology, and Age Model Adjustments

The complete record spanned 0 to 2,720 cm (4.7–122.1 ka) and was 92% complete. Sediments at the core top and bottom were not entirely lacustrine. The bottom 1 m section was composed of massive, poorly sorted sand and pebbles, suggesting a higher-energy environment that was potentially fluvial. Infrared-stiumulated luminescence results indicated that these coarse deposits dated to the Last Interglacial (124 ± 8 ka). Pollen deposited into the basin was not well preserved until ~2,300 cm (103.7 ka). There were five notable core gaps (>20 cm) resulting from a lack of recovery and highly disturbed sediments. Those that impacted pollen analysis are shown in Figure 4, with horizons and ages detailed in the supporting information.

Our weighted mean age results above the top-most ^{14}C date (11.6 ka, 152 cm) sediment showed evidence of frequent lake desiccation, and pollen is not well preserved above ~14.6 ka. This prevented analysis of MIS 1. We show data (e.g., pXRF, LOI, MS, and charcoal) obtained from these upper sediments to 10 ka where possible but keep the scope of our interpretation to the period that spanned 120 ka to the Pleistocene-Holocene transition (~15 ka).

4.2. Physical and Geochemical Markers: Observations and Proxy Interpretation

Biogenic silica (BSi) and bulk organic content from LOI yield insight about the basin's autochthonous, biologic deposition history (Conley & Schelske, 2002; Dean, 1974). In prior work, bulk organic content was hypothesized to be a record of lake paleoproductivity (BSi), based upon the two proxies' strong correlation ($r = 0.81$; Figure 3a; Glover et al., 2017).

Molar C/N values from 8 to 10 signal a dominant phytoplankton source, while values ≥20 represent organic matter from terrestrial plants (Curtis et al., 2010; Meyers, 1994; Overpeck et al., 2013; Thevenon et al., 2012). Intermediate C/N values that range 10–20 generally indicated combined autochthonous (i.e., aquatic) and allochthonous (i.e., terrestrial) sources of organic deposition. In the Lower Bear Lake record west of

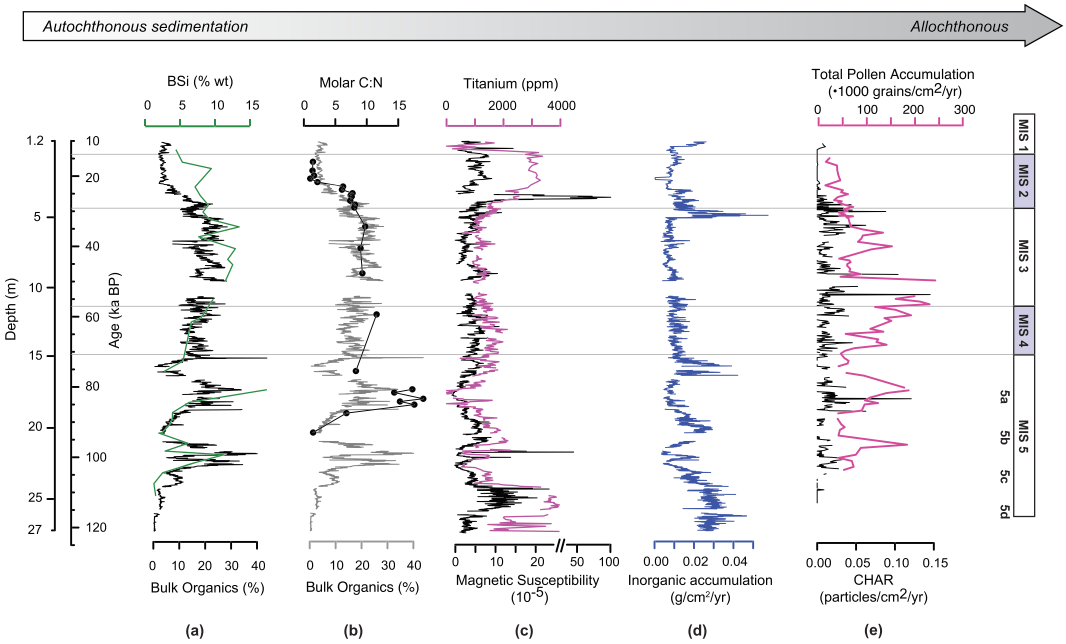

Figure 3. Proxy data related to BDL12 deposition, and basin erosion across Marine Isotope Stages (MISs) 5–1. Proxy data are arranged left to right from those that suggest authochthonous deposition toward allocthonous deposition. (a) Bulk organic content (%) derived from loss on ignition and biogenic silica (% wt). (b) Bulk organic content (%) and molar C:N data points. (c) Titanium (Ti, ppm) and magnetic susceptibility (MS). (d) Inorganic accumulation over time (g/cm^2/year). (e) Charcoal accumulation rate (CHAR, particles/cm^2/year) and Total pollen accumulation (PAR, 1000 grains/cm^2/year).

Baldwin Lake (Figure 1), molar C/N ≥ 9 indicated Holocene-age pluvial events that enhanced surface runoff and allochthonous organic deposition within the catchment (Kirby et al., 2012).

Molar C/N ranged from 1.02 to 18.97 during the period measured (93–15 ka, Figure 3b). C/N was ≤10 for most of the sequence, suggesting autochthonous deposition dominated organic deposition. Higher C/N values (14.5–19) occur from 85 to 81 ka during MIS 5a, where organic content was also relatively high (20–35%), suggesting enhanced organic deposition from Baldwin's watershed and terrestrial plants.

Additional measures of allochthonous deposition included titanium (Ti) and magnetic susceptibility (MS, Figure 3c; Dearing, 1999; Kylander et al., 2011). We assume that Ti was lithogenic and washed into the lake, with values from 196 to 3,968 ppm. MS was related to ferrogenous sedimentation (Thompson & Oldfield, 1986) and ranged from -0.9×10^{-5} to 25×10^{-5} SI throughout the record, with one 100.6×10^{-5} SI excursion centered 26.6–25.8 ka. The rate of inorganic accumulation fluctuated over time between 0.0003 and 0.0576 g/cm^2/year (mean = 0.0152 g/cm^2/year), with the greatest inorganic transport into the basin at 121.3–104.4, 76.1–73.5, 31.8–29.7, and 10.9–10.2 ka with flux rates ≥0.02 g/cm^2/year.

4.3. Ecological Markers: Observations and Proxy Interpretation

4.3.1. Charcoal

Charcoal data spanned ~115.1–9.1 ka (2,556–100 cm), with a few coring and analytic gaps. Results until 10 ka are reported here as CHAR (Figure 3e), as changes in relative sediment influx can affect charcoal particle deposition (Conedera et al., 2009). Values ranged from 0 to 0.15 particles/cm^2/year, and charcoal was absent in 28% of our samples.

4.3.2. Pollen Identification, Accumulation, and Zonation

A total of 42 fossil pollen taxa were identified and counted to family or genus level, including aquatic, herbs and shrubs (i.e., nonarboreal), and arboreal taxa. CONISS zonation produced four major zones; most had sublevels (Figure 4). Table 1 outlines the depth and age of each subzone, listing the common taxa and their relative abundance. PAR (Figure 3e) varied from 15 to 239·10^3 grains/cm^2/year from 103.8 to 14.6 ka, with the highest accumulation at the MIS 4/3 transition (~63–54 ka). Pollen zonation based upon taxa percent changes is shown in Figure 4 and a synoptic summary in Table 1.

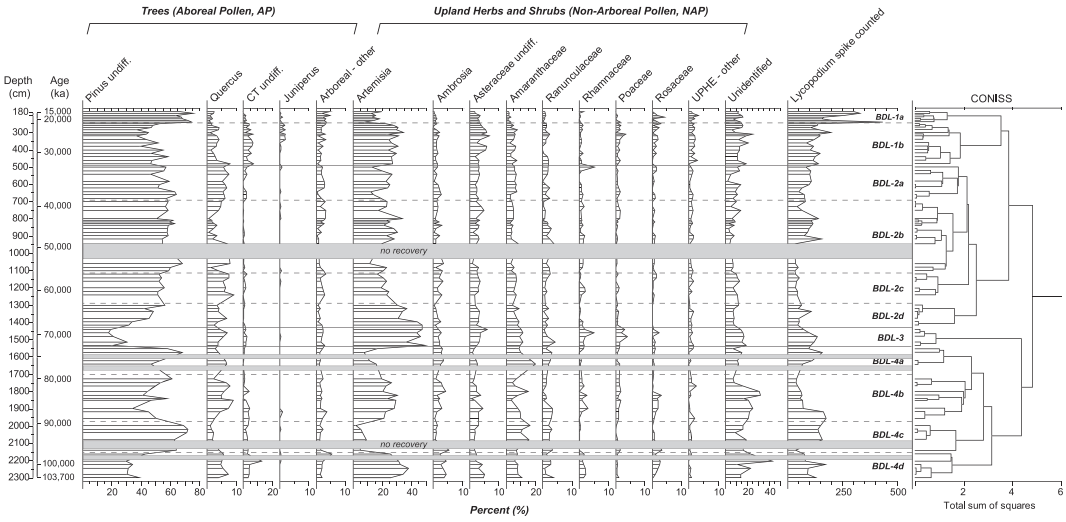

Figure 4. Fossil pollen major taxa and groups for Baldwin Lake (BDL12) from ~108.5 to 15 ka. Horizontal lines indicate sampled horizons. Gray bars indicate horizons of no recovery that were ≥20 cm. Sediment from 2,164–2,184 cm was consumed for IRSL dating. See Table 1 for synoptic description of pollen found in zones.

Table 1
Fossil Pollen Zonation Summary for BDL12, With Taxa Arranged in Order From Most to Least Abundant Within Each Zone

Zone	Depth (cm) and Age (ka)	Taxa range (minimum-maximum %; average), other notes
BDL-1a	180–245 14.6–23.1	*Pinus* (62–75%; 70%) *Artemisia* (8–20%; 14%) undiff. Asteraceae (2–4%; 3%) Arboreal-other (2–5%; 3%) unknowns (2–5%, 3%) Amaranthaceae (1–3%, 2%) *Quercus* (1–3%, 2%) Herbs and shrubs-other (1–3%, 1%) CT (0–2%, 1%) *Ambrosia* (0–1%, 1%)
BDL-1b	245–490 23.1–31.1	*Pinus* (35–59%, 47%) *Artemisia* (22–35%, 27%) Amaranthaceae (2–8%, 5%) CT (1–7%, 4%) undiff. Asteraceae (2–7%, 4%) *Quercus* (1–7%, 3%) unknowns (2–8%, 5%) Arboreal-other (0–3%, 2%) Herbs and shrubs-other (0–3%, 2%) *Ambrosia* (0–2%, 1%)
BDL-2a	490–690 31.1–38.1	*Pinus* (47–64%, 56%) *Artemisia* (12–27%, 20%) *Quercus* (5–8%, 6%) Amaranthaceae (3–7%, 6%) undiff. Asteraceae (2–3%, 3%) unknowns (0–4%, 2%) Arboreal-other (0–3%, 2%) *Ambrosia* (0–3%, 2%) CT (0–3%, 1%) Herbs and shrubs-other (0–2%, 1%)
BDL-2b	690–1,110 38.1–56.0 gap 49.9–53.1 ka	*Pinus* (51–63, 58%) *Artemisia* (17–34%, 25%) Amaranthaceae (2–8%, 4%) *Quercus* (1–7%, 3%) undiff. Asteraceae (2–5%, 3%) *Ambrosia* (0–3%, 1%) Arboreal-other (0–3%, 2%) unknowns (0–4%, 2%) CT Herbs and shrubs-other (0–2%, 1%) TCT (0–1%, 0%)
BDL-2c	1,110–1,290 56.0–63.0	*Pinus* (51–68%, 56%) *Artemisia* (12–24%, 20%) *Quercus* (1–9%, 6%) Amaranthaceae (3–7%, 6%) *Ambrosia* (1–4%, 2%), undiff. Asteraceae (1–4%, 3%) unknowns (2–4%, 3%) Arboreal-other (1–3%, 2%) CT (0–2%, 1%) Herbs and shrubs-other (0–2%, 1%)
BDL-2d	1,290–1,430 63.0–68.5	*Pinus* (32–56%, 43%) *Artemisia* (31–48%, 37%) Amaranthaceae (4–9%, 7%) *Quercus* (3–7, 4%) undiff. Asteraceae (2–3%, 3%) unknowns (1–3%, 2%) *Ambrosia* (0–3%, 1%) Aboreal-other (1–2%, 1%) Herbs and shrubs-other (0–2%, 1%) CT (0–1%, 0%)
BDL-3	1,430–1,540 68.5–72.8	*Artemisia* (37–50%, 45%) *Pinus* (16–31%, 22%) Amaranthaceae (9–12%, 10%) unknowns (5–6%, 6%) *Quercus* (4–7%, 5%) undiff. Asteraceae (3–6%, 4%) *Ambrosia* (2–3%, 2%) Arboreal-other (2–3%, 2%) CT (1–2%, 2%) Herbs and shrubs-other (0–2%, 1%)
BDL-4a	1,540–1,700 72.8–79.1 gap 74.4–75.4 ka 77.0–78.1 ka	*Pinus* (47–68%, 57%) Amaranthaceae (9–20%, 14%) *Artemisia* (8–17%, 13%) *Quercus* (3–7%, 5%) *Ambroisia* (3–4%, 3%) unknowns (3–5%, 4%) undiff. Asteraceae (1–3%, 2%) Arboreal-other (1–2%, 1%) Herbs and shrubs-other (0–1%, 1%) CT (0–1%, 0%)
BDL-4b	1,700–1,970 79.1–89.6	*Pinus* (34–61%, 48%) *Artemisia* (20–30%, 22%) Amaranthaceae (4–15%, 8%) *Quercus* (2–9%, 6%) unknowns (2–11%, 6%) *Ambrosia* (1–4%, 2%) undiff. Asteraceae (1–5%, 2%) Arboreal-other (1–4%, 2%) CT (0–4%, 2%) Herbs and shrubs-other (0–3%, 1%)
BDL-4c	1,970–2,150 89.6–96.9 gap 93.4–95.7 ka	*Pinus* (62–72%, 68%) Amaranthaceae (7–16%, 12%) *Artemisia* (2–9%, 6%) unknown (3–6%, 5%) *Ambrosia* (1–5%, 2%) *Quercus* (1–4%, 2%) undiff. Asteraceae (2–3%, 2%) CT (1–3%, 2%) Arboreal-other (1–2%, 1%) Herbs and shrubs-other (0–1%, 0%)
BDL-4d	215–2,300 96.9–103.8 gap 97.6–98.5 ka	*Pinus* (30–43%, 35%) *Artemisia* (26–38%, 31%) Amaranthaceae (6–10%, 8%) *Quercus* (4–7%, 5%) CT (3–12%, 5%) unknown (3–15%, 7%) undiff. Asteraceae (2–5%, 4%) *Ambrosia* (2–4%, 3%) Arboreal-other (1–5%, 2%) Shrubs and herbs-other (0–1%, 1%)

Note. CT = Cuppressaceae-Taxaceae families; "undiff." = undifferentiated. Taxa groups (e.g., "other") are detailed in the supporting information. Complete data set of ungrouped taxa, including those that averaged <3% in all zones, is available at the Neotoma Paleoecological Database.

Overall, *Pinus* (pine) was the most abundant pollen type in most zones and subzones of our record, peaking at 76% at ~15.6 ka, and with its minimum of 17.8% at 69.7 ka. Within the nonarboreal pollen (NAP) group, *Artemisia* reached a maximum of 49.6% at 72.5 ka, with a minimum of 2.0% at 90.7 ka. Other taxa that were the most prevalent in the record included Amaranthaceae (goosefoot, 1–19%), *Quercus* (oak, 1–9%), Cupressaceae-Taxaceae (CT, cypress-yew families, 0–8%), undifferentiated Asteraceae (daisy family, 1–6%), and *Ambrosia* (ragweed, 0–5%). Further environmental interpretation that is integrated with other proxy data follows in section 5.

5. Discussion

Here, we focus on insights from the Baldwin Lake record on linkages between erosion, wildfire, and vegetation in Southern California's subalpine landscape since 120 ka and how they responded to climatic forcing. We discuss environmental response to climatic forcing based upon the following assumptions. First, we used the Lisiecki and Raymo (2005) MIS boundaries to frame our figures, site interpretation, and discussion of glacial (odd-numbered MISs) versus interglacial (even-numbered MISs) periods. Second, we use June 30° N latitude insolation values from the Laskar et al. (2004) solution to explore the impact of orbital forcing on the processes and change that our proxy data represent. Regional summer radiation would have directly influenced light availability during the growing season for algae and plants (Crucifix & Loutre, 2002) and impacted moisture delivery to Southern California (Kirby et al., 2006). Prior work showed these relationships with an age model tuned to this insolation data set, based upon the assumption that primary productivity in Baldwin Lake responded immediately to shifts in summer light availability from MIS 5d until the onset of MIS 2 (Glover et al., 2017). While we do not discount this potential forcing relationship between insolation and paleoproductivity, we feel the untuned age model more appropriate for discussing the pace and timing of terrestrial change and processes.

5.1. Weathering and Erosion in the SBM From 120–15 ka

Biologic and detrital deposition fluctuated and are often opposed to each other throughout the Baldwin Lake record. Periods dominated by allochthonous deposition were signaled with heightened MS, Ti, and inorganic flux into the basin and low values for bulk organics and BSi (Figure 3). Cool, glacial-like conditions with enhanced weathering and erosion prevailed at the start of the record (the MIS 5e/5d transition, ~121–105 ka), the end of MIS 5a (~76–71 ka), and the transition from MIS 3 into the last glacial and MIS 2 (~32–14 ka). The shift between productive and unproductive lake states was the most pronounced during MIS 5. These reversals are high amplitude and rapid relative to the rest of the record, with transitions that ranged 6.8–11.5 kyr between the two lake states.

The molar C/N data set also reflected this high-amplitude change from MIS 5b to its maximum centered at MIS 5a, where values ≥10 suggested enhanced allochthonous sources for organic material. We had employed selective C/N analysis to explore (1) its correlation with bulk organics and (2) if high values would signal a terrestrial source of either organic matter or nutrient loading (Ampel et al., 2008; Conley & Schelske, 2002). MIS 5a was also a time that lake level fluctuated on 10^4 year scales, with noteable fluctuations at 85.8 and 82.8 ka (Glover et al., 2017). Despite this variation in lake size, organics and C/N remained closely tied throughout the record (Figure 3b, $r = 0.81$), suggesting that weathering processes also contributed to an organic record that we previously interpreted as one of paleoproductivity.

The MIS 5/4 transition (~71 ka) was the onset of a weaker basin weathering regime that lasted through MIS 4 and MIS 3. This interpretation is consistent with other work in the SBM that shows active alluvial aggradation in its southwestern flank at the onset of MIS 4, then quiescence during MIS 3–2 (Owen et al., 2014). Baldwin MS values were <10 10^{-5} SI, inorganic flux was low until ~32 ka, and the lake moderately productive with bulk organic content averaging 18.0%.

Proxy data we examine together for basin erosion (e.g., Ti, MS, and inorganic flux) still had excursions independent of each another, such as the maxima in MS and inorganic flux (Figures 3c and 3d). We also saw evidence that basin relationships changed over time, such as the stronger correlation between Ti and MS prior to the last glacial ($r = 0.75$), compared to the entire record ($r = 0.29$). Antiphased Ti and MS are most apparent during the Last Glacial Maximum (LGM; Figure 3c), and low inorganic flux suggests a period of weak erosion in the cold, forested lake basin. Cold glacial conditions have been shown to support elevated Ti

levels in lake records, an element that can bind to clay and finer particles to concentrate in lake sediment (Minyuk et al., 2006). We found no apparent relationship between CHAR and MAR ($r = -0.08$), measures both based upon basin sedimentation rate. We thus interpret CHAR data as a measure of wildfire activity over time in the Baldwin watershed that was largely independent of erosion.

5.2. Wildfire and Vegetation in Subalpine California From 110 to 15 ka

Charcoal deposition was low during MIS 5 and MIS 2 (mean = 0.009 and 0.001 particles/cm^2/year, respectively) relative to the interval in-between (Figure 3e). Similar to sedimentological and geochemical proxies discussed, the PAR for the sum of all pollen types demonstrated high-amplitude, cyclic change during MIS 5 (Figure 3e). However, there was not a strong relationship between PAR (potential vegetation/fuel) and CHAR ($r = 0.39$). During the last glacial, CHAR decreased to values <0.01 by 27.2 ka, suggesting climatic conditions that did not support subalpine wildfire. Pollen concentration also remained low throughout MIS 2 (<75 10^4 grains/cm^2/year), though the percent values of different taxa suggest a shift in forest composition during MIS 2, possibly due to the lack of wildfire. *Juniperus* was counted continuously from 27.9–20.9 ka, and *Pinus* reached values 74% at 22.4 ka and remained above 64% for the rest of the record.

Sedimentological and geochemical proxy data in our record had intermediate values that suggest a phase of weak basin weathering, and perennial lake conditions during MIS 4–3. By contrast, charcoal and pollen data suggest ecological processes that were independently active and dynamic. Both concentration and percent calculations suggest that the landscape was predominantly open sagebrush at the MIS 5/4 transition. Parsing total pollen concentration into nonarboreal (NAP) and arboreal (AP) components showed that NAP exceeded AP for ~6 kyr and reached its maximum in the record ($86.6 \cdot 10^4$ grains/cm^2/year). Our lowermost pollen samples from 103.7 to 99.4 ka also show NAP (average = $34.2 \cdot 10^4$ grains/cm^2/year) exceeding AP (average = $25.5 \cdot 10^4$ grains/cm^2/year) during MIS 5d–5c. This "sage expansion" may signal climate conditions that induced tree line migration toward lower elevations, as documented in other long subalpine records in the North American West (e.g., Star Marsh, Herring & Gavin, 2015).

Total pollen concentration increased throughout MIS 4 as trees repopulated the basin and the landscape transitioned to woodland, then forest. *Pinus* remained the dominant taxon counted for most of MIS 3 and may have contributed to landscape stability. Despite the low variation in the vegetation assemblage that the pollen percent data suggested, pollen concentration was highly variable. This includes PAR maxima in early MIS 3 at 56.4 ka ($227 \cdot 10^4$ grains/cm^2/year) and 49.6 ka ($239 \cdot 10^4$ grains/cm^2/year), with a rapid decrease at 48.5 ka (Figure 3e). Charcoal deposition was more active during MIS 3 (CHAR mean = 0.014 particles/cm^2/year), with peaks at 55.6 ka (0.145 particles/cm^2/year) and 49.9 ka (0.104 particles/cm^2/year). These suggest that the most dynamic time for wildfire and high vegetation density was MIS 4 to MIS 3.

5.3. Global Climatic Drivers in Southern California From 120 to 15 ka

Prior work on Baldwin Lake hypothesized that summer insolation was the primary influence on lake paleoproductivity reflected in measures of bulk organic matter over long time scales (10^4–10^5 year) from MIS 5e to the MIS 2/1 transition (Glover et al., 2017). Our coarse C/N sampling suggested that allochthonous organic and/or nutrient input also contributed to bulk organic matter. As such, we explore here climatic drivers for terrestrial and ecological change in the Baldwin Lake basin with an untuned age model that was not based upon the assumption that insolation and bulk organic matter were tied. Both models were within ±2 kyr of each other for most of the record (98–10 ka) and diverged up to 5.5 kyr during MIS 5c and 5d. These offsets were comparable to the range of error in our untuned age model (mean error = ±4.9 kyr for MIS 5), which was based upon IRSL dating and Bayesian modeling in the lower parts of the core.

We found that shifts in basin erosion and weathering on coarse time scales (10^4–10^5 kyr) created different lake states, with the most rapid (6.8–11.5 kyr) alternations between biologic and detrital deposition during MIS 5. Summer insolation at 30°N from 120–15 ka also exhibited its most rapid and highest-amplitude shifts during MIS 5. Variation ranged 448–537 W/m^2, and the time between maxima and minima was ≤11 kyr (Figures 5b and 5c). Insolation showed apparent asynchronicity with our bulk organic content when plotted with our untuned age model (Figure S3) but remained within the age model's range of error. Summer insolation was less variable after 71 ka and fluctuated between 465–515 W/m^2 and a range of 50 W/m^2, compared to MIS 5 (an 89 W/m^2 range). During this reduced seasonality during MIS 4–3, Baldwin Lake remained perennial and landscape erosion was minimal. Its last shift to an unproductive lake occurred in MIS 2, and basin

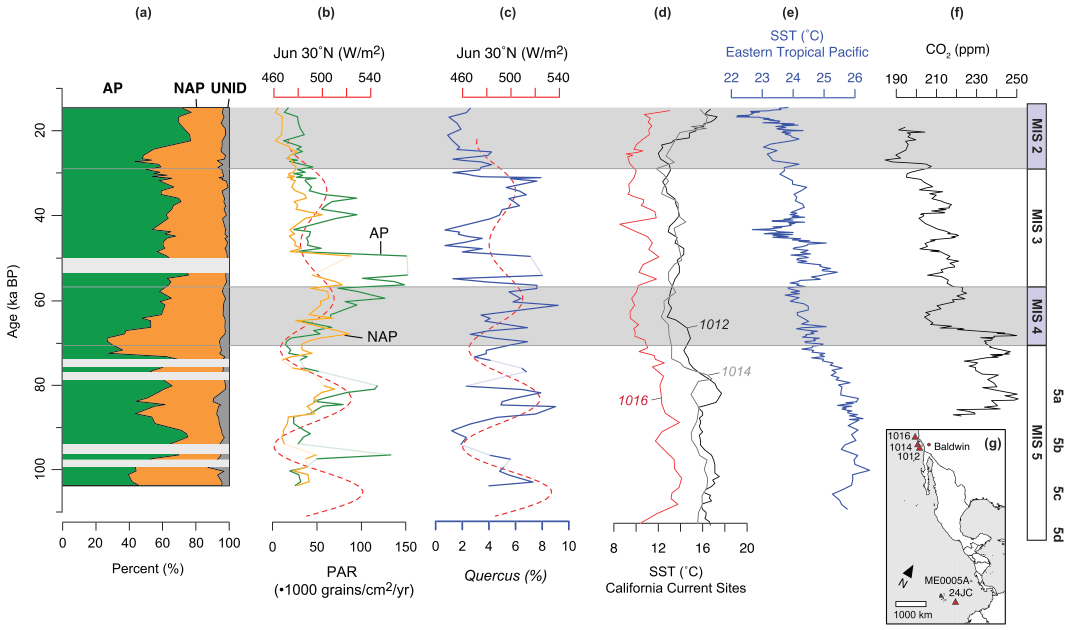

Figure 5. BDL12 fossil pollen data and potential climatic drivers. (a) Proportion of arboreal pollen (AP) to nonarboreal pollen (NAP) and unidentified grains (UNID). (b) AP and NAP pollen accumulation rate (PAR) with 30°N summer insolation (Laskar et al., 2004). (c) *Quercus* (oak) pollen percent highlights millennial-scale variability in the vegetation record, with 30°N summer insolation. (d) Sea surface temperatures (SSTs) from paleorecords 1,012, 1,014, and 1,016 off the coast of Southern California (Herbert et al., 2001). (e) SSTs from an eastern tropical Pacific paleorecord (Dubois et al., 2011). (f) Record of global carbon dioxide (Ahn & Brook, 2008).

desiccation followed in early MIS 1. We hypothesize that insolation was an important climatic driver on the depositional processes that influenced lake state over 10^4 to 10^5 year time scales, including basin erosion and lake productivity.

We have shown that wildfire and vegetation change do not have a straightforward relationship to each other. PAR for both AP and NAP was highly cyclic during MIS 5 (Figure 5b) and ~7–8 kyr between PAR maxima and minima. Fluctuations in AP and NAP during MIS 5 appear offset from summer solar radiation, though this is within the range of error of our untuned age model. The rise of AP that began ~65 ka and lasted until its maximum at 50 ka, then rapidly declined, does not follow the intermediate insolation trends that characterize MIS 3. Higher percentages of *Quercus* have been interpreted as oak expansion during warmer temperatures in Southern California and observed to have millennial-scale oscillations since MIS 5 (Heusser, 2000). Our *Quercus* record followed the apparent trend of summer insolation, though with smaller-order millennial-scale shifts. Compared to the Santa Barbara Basin record, these *Quercus* fluctuations occurred on similar temporal time scales yet were lower in amplitude (Figure 5c). This suggests that climatic drivers on finer temporal scales ($\leq 10^4$ year) affected vegetation growth and composition in Big Bear Valley.

We compare our pollen record briefly against records with $\leq 10^4$ year resolution that are proxy records for regional and global climate drivers, including sea surface temperature (SSTs) and CO_2 concentrations. These records include a series of marine cores off the coast of California (Figure 5d) that show north-south SST differences since MIS 5, due to variable strength of the California Current (Herbert et al., 2001). Southern California SSTs had a tendency to warm earlier (~3–5 kyr) than northerly records during glacials. The MIS 5a maxima for core 1012 occurred during MIS 5a, coeval with a summer insolation peak and higher AP. SSTs at 1,012 also warmed in advance of other offshore California records during the first half of MIS 4, when CO_2 concentrations also peaked (~250 ppm at ~68 ka, Figure 5f) and sagebrush expansion overtook forest in the SBM. A potential CO_2-vegetation linkage did not hold during MIS 3, however, where 3–4 kyr oscillations in CO_2 were out of phase with PAR.

SST fluctuations in the tropical eastern Pacific are responsible for an important area for El Niño Southern Oscillation generation (Dubois et al., 2011; Figure 5e). Presently, winter precipitation delivery to

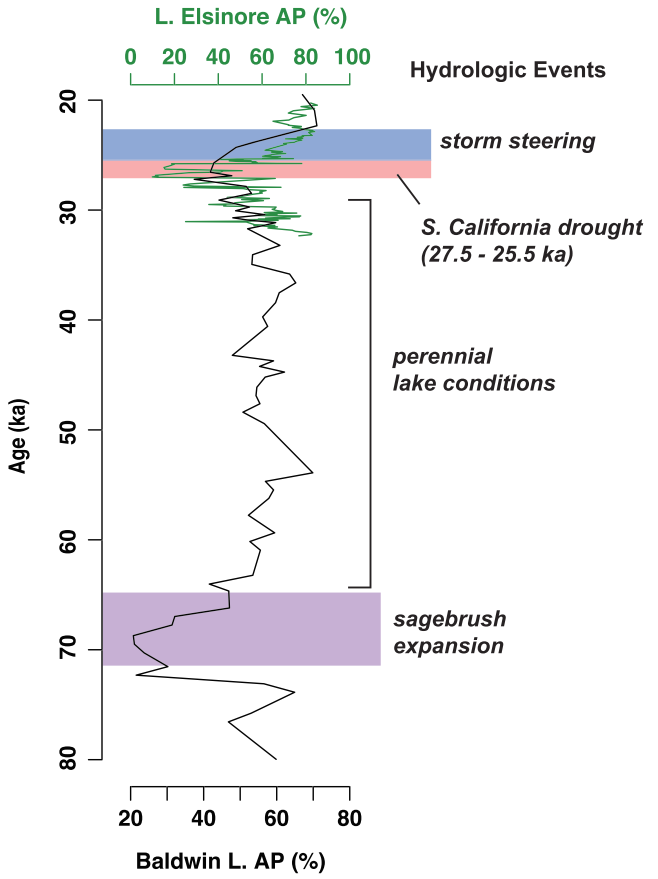

Figure 6. Comparison of Baldwin Lake and Lake Elsinore (Figure 1) arboreal pollen, highlighting Southern California paleohydrology across the last glacial period (MIS 2).

California is weakly connected to the SST variability that El Niño Southern Oscillation induces (Seager et al., 2019). Global CO_2, here shown with an Antarctic record, was ≥220 ppm before declining to ≤220 ppm until the LGM (Ahn & Brook, 2008; Figure 5f). While these drivers may have worked in concert to produce the set of climatic conditions and environmental response in our record, there is no direct linkage between vegetation growth and SSTs nor CO_2 throughout the majority of the record. Meanwhile, much of our proxy data followed the broader trend of summer insolation over long (10^5 year) time scales.

5.4. Submillennial-Scale Hydrologic Forcing in Southern California During MIS 4–2

We have established that the latter half of MIS 4 and the duration of MIS 3 (~65–30 ka) was a time when summer insolation exhibited the least variation (Figures 3b and 3c) and the landscape conditions in the SBM included expanded coniferous forest, productive lake conditions, and weak basin weathering. Despite relatively stable "background" conditions that followed insolation trends, several of our proxy data sets demonstrated millennial-scale (10^3 year) and submillennial-scale ($<10^3$ year) variability that may indicate hydrologic variation on similar time scales. This was first evident in our highly resolved (i.e., every 1 cm) bulk organic data from MIS 3 (Figure 3a), which we hypothesized to be a response to Dansgaard-Oeschgar events (Glover et al., 2017; Kirby et al., 2006). Pollen and charcoal proxies in our record, though analyzed at a coarser resolution, supported the possibility of submillennial hydrologic forcing with ~10^3 year perturbations from the long-term solar trend (Figure 5c), a pattern also evident in Santa Barbara Basin pollen data (Heusser, 2000).

No linear relationship nor phasing existed between the vegetation presence and wildfire inferred from our PAR and CHAR data sets. However, the combination of submillennial hydrologic variability and closed *Pinus*-dominated forest cover during this ~35 kyr period may have been the environmental conditions necessary to support wildfire in the SBM. During the LGM (26–19 ka; Clark et al., 2009), other regional paleorecords have demonstrated this hydrologic dynamism. Lake Elsinore (Figure 1) *Juniperus* pollen declined during drought from 27.5 to 25.5 ka (Figure 6; Heusser et al., 2015). *Pinus* pollen at Baldwin Lake declined for ~7–8 kyr in the lead-up to this drought, with its MIS 2 minimum in AP coeval with Elsinore's drought onset (43% at 27.0 ka; Figure 6). The difference in Elsinore AP ranged 10–85% from 29 to 20 ka, while Baldwin AP exhibited lower-amplitude fluctuations from 43% to 77% at this time (Figure 6), suggesting that the drought impact on mountain vegetation was muted compared to lower-elevation ecosystems. AP increased at both Elsinore and Baldwin starting ~24 ka, indicating that intense moisture delivery to Southern California resumed during the LGM (e.g., Oster et al., 2015).

European pollen sequences that span multiple glacial-interglacial cycles showed that forest expansion *generally* peaked with summer insolation maxima, rather than times of ice sheet wasting. In the Mediterranean biomes of southern Europe and Anatolia, however, moisture availability impacted the expansion of sclerophyllus taxa, such as oak, more than enhanced light and warmth brought with mid-June insolation (Pickarski et al., 2015; Tzedakis, 2005). Thus, high analytic resolution (i.e., <200 year) in pollen data can highlight centennial-scale vegetation perturbations that deviate from orbital trends and are hydrologically driven, particularly in Mediterranean ecosystems (Tzedakis, 2005). Similar work at this resolution has highlighted hydrologic change in Lake Elsinore during the last glacial (Figure 6; Heusser et al., 2015), and rapid (10^1–10^2 year) *Pinus* excursions in the Santa Barbara Basin that were related to moisture increases across the MIS 2/1 transition (Heusser & Sirocko, 1997). This highlights the continued need for similarly resolved pollen analysis in Southern California records prior to the LGM, in order to better understand the nature, scale, and cyclicity of paleohydrologic change.

6. Conclusions

We developed a multiproxy record for Baldwin Lake in the SBM of Southern California, which allowed us to examine variation in erosion, wildfire, and vegetation change from ~120 to 15 ka. During MIS 5, high-amplitude shifts in organic content and basin weathering signaled a lake that alternated between productive (autochthonous) and unproductive (allocthonous deposition) states. Forest expansion and contraction, as indicated by arboreal pollen counts, were out of phase with both low charcoal counts and weathering proxy data. Reduced tree line and sagebrush steppe expansion in early MIS 4 (~71–65 ka) occurred at the onset of a weak weathering phase that continued throughout MIS 3. MIS 3 also sustained coniferous forest in the SBM, a productive lake, and variable wildfire. Millennial- to submillennial-scale variability was present in several proxies, suggesting a hydrologic forcing mechanism. Allochthonous sources dominated deposition in Baldwin Lake during MIS 2, while charcoal and pollen concentrations declined to their lowest sustained levels in the record. Arboreal pollen still signaled rapid forest expansion ~24 ka, coeval with wetter conditions at Lake Elsinore (Kirby et al., 2018), and other paleorecords in Southern California (Oster et al., 2015).

Taken together, these proxy data show that over multiple glacial-interglacial cycles, the interactions between terrestrial processes and climate drivers were complex in Southern California. Despite the apparent cyclicity of certain proxy data sets (e.g., pollen), it was challenging to discern clear cause-and-effect relationships between ecological process, sedimentation, and insolation that were persistent for the entirety of the Baldwin Lake record. Relationships that persisted for the duration our record, such as the link between summer insolation, biologic productivity, and changing lake state, were most apparent on coarse time scales ($\geq 10^4$ yr).

The impact of summer insolation on ecological processes in the SBM was also less clear. Charcoal and pollen percentages tended to follow *background* radiation conditions (10^4–10^5 year; Figures 5b and 5c), with several shorter time scale (10^3 year) perturbations. Arboreal pollen data showed this best, with forest expansion that generally followed summer light availability, but with smaller-scale ($\leq 10^3$ year) variations that may reflect hydroclimatic forcing. This highlights the continued need for highly resolved (~200 year resolution) terrestrial proxy data in Southern California prior to the LGM, in order to better understand (1) the influence of marine drivers on terrestrial processes and (2) hydroclimatic variation on submillennial scales.

Such hydrologic variability has been shown to induce rapid vegetation change in long (>100 kyr) pollen records from Eurasia's Mediterranean biome (Tzedakis, 2005). This propensity for rapid change means that climate change during the rest of the 21st century could induce significant vegetation shifts in California. Seager et al. (2019) projected that North America's Mediterranean region will mostly experience enhanced winter precipitation, though higher temperatures and evaporative demand in Southern California will produce a net decrease in effective precipitation. This could convert the region to subtropical steppe or subtropical desert (Seager et al., 2019), and our record showed that this has happened in the past. Widespread *Pinus* sp. mortality has been impacting the Sierra Nevada since 2000 (Stevens & Corina, 2016; USDA Forest Service, 2005) alongside vegetation thermophilization (Stevens et al., 2015). Upward vegetation migration has been documented elsewhere in the Transverse Ranges (Kelly & Goulden, 2008). This suggests that a widespread vegetation response to anthropogenic climate change is already happening in California's coniferous forests.

Acknowledgments
Grants and fellowships from the Society of Woman Geographers, UCLA Graduate Division Dissertation Year Fellowship, and UCLA La Kretz Center for California Conservation Science to K. C. G. supported the analyses conducted in this work. Additional funding came from the UCLA Department of Geography John Muir Memorial Endowment. The authors declare no conflicts of interest. Baldwin Lake sedimentary, geochemical, and charcoal data are archived in the NOAA National Centers for Environmental Information (https://www.ncdc.noaa.gov/paleo/study/28750). Full pollen counts are also available at the Neotoma Paleoecology Database (apps.neotomadb.org/Explorer/?datasetid=46603), and we are grateful to Eric Grimm for his advice on taxonomic interpretation and archiving these data. We thank Larry Winslow and Scott Eliason for their insight and assistance during fieldwork. We also thank several students for assistance in the lab including Lauren Brown, Elaine Chang, Tamryn Kong, Alec Lautanen, Victor Leung, Scott Lydon, Setareh Nejat, Alex Pakalniskis, and Marcus Thomson. K. C. G. thanks the Past Global Changes (PAGES) working group for support to present an earlier version of this research at the "Fire Prediction Across Scales" workshop and feedback from the research community. Reviews and comments from Andrew Cohen, James Russell, and an anonymous reviewer greatly improved the manuscript.

References

Ahn, J., & Brook, E. J. (2008). Atmospheric CO2 and climate on millennial time scales during the Last Glacial Period. *Science*, *322*(5898), 83–85. https://doi.org/10.1126/science.1160832

Ampel, L., Wohlfarth, B., Risberg, J., & Veres, D. (2008). Paleolimnological response to millennial and centennial scale climate variability during MIS 3 and 2 as suggested by the diatom record in Les Echets, France. *Quaternary Science Reviews*, *27*, 1493–1504. https://doi.org/10.1016/j.quascirev.2008.04.014

Anderson, R. S., & Koehler, P. A. (2003). Modern pollen and vegetation relationships in the mountains of southern California, USA. *Grana*, *42*, 129–146. https://doi.org/10.1080/00173130310009949

Arianoutsou, M., Leone, V., Moya, D., Lovreglio, R., Delipetrou, P., & Heras, J. (2012, Dordrecht). Management of threatened, high conservation value, forest hotspots under changing fire regimes. In F. Moreira, M. Arianoutsou, P. Corona, & J. De las Heras (Eds.), *Post-fire management and restoration of southern European forests*, (pp. 257–291). Dordrecht, Netherlands: Springer Netherlands.

Bailey, R. G. (2009). *Ecosystem geography: From ecoregions to sites*, (2nd ed.). New York: Springer.

Ballard, J. P. (2009). *A lateglacial paleofire record for east-central Michigan*. Cincinnati, OH: University of Cincinnati.

Barbour, M. G., & Billings, W. D. (Eds) (2000). *North American terrestrial vegetation*, (2nd ed.). Cambridge: Cambridge Univ. Press.

Bedsworth, L., Cayan, D., Franco, G., Fisher, L., Ziaja, S., 2018. Statewide summary report. California's Fourth Climate Change Assessment. (No. SUMCCCA4-2018– 013). California Governor's Office of Planning and Research, Scripps Institution of Oceanography, California Energy Commission, California Public Utilities Commission.

Bennett, K. D., & Willis, K. J. (2001). Pollen. In J. P. Smol, H. J. B. Birks, W. M. Last, R. S. Bradley, & K. Alverson (Eds.), *Tracking environmental change using lake sediments*, (pp. 5–32). Dordrecht: Kluwer Academic Publishers.

Blaauw, M., & Christen, J. A. (2011). Flexible paleoclimate age-depth models using an autoregressive gamma process. *Bayesian Analysis*, *6*, 457–474. https://doi.org/10.1214/11-BA618

Clark, P. U., Dyke, A. S., Shakun, J. D., Carlson, A. E., Clark, J., Wohlfarth, B., et al. (2009). The Last Glacial Maximum. *Science*, *325*(5941), 710–714. https://doi.org/10.1126/science.1172873

Conedera, M., Tinner, W., Neff, C., Meurer, M., Dickens, A. F., & Krebs, P. (2009). Reconstructing past fire regimes: Methods, applications, and relevance to fire management and conservation. *Quaternary Science Reviews*, *28*, 555–576. https://doi.org/10.1016/j.quascirev.2008.11.005

Conley, D. J., & Schelske, C. L. (2002). Biogenic Silica. In J. P. Smol, H. J. B. Birks, W. M. Last, R. S. Bradley, & K. Alverson (Eds.), *Tracking environmental change using lake sediments*, (pp. 281–293). Dordrecht: Kluwer Academic Publishers.

Crucifix, M., & Loutre, F. (2002). Transient simulations over the last interglacial period (126-115 kyr BP): Feedback and forcing analysis. *Climate Dynamics*, *19*, 417–433. https://doi.org/10.1007/s00382-002-0234-z

Curtis, C. J., Flower, R., Rose, N., Shilland, J., Simpson, G. L., Turner, S., et al. (2010). Palaeolimnological assessment of lake acidification and environmental change in the Athabasca Oil Sands Region, Alberta. *Journal of Limnology*, *69*, 92–104. https://doi.org/10.3274/jl10-69-s1-10

Davis, O. K. (1999a). Pollen analysis of Tulare Lake, California: Great Basin-like vegetation in Central California during the full-glacial and early Holocene. *Review of Palaeobotany and Palynology*, *107*, 249–257. https://doi.org/10.1016/S0034-6667(99)00020-2

Dean, W. E. (1974). Determination of carbonate and organic matter in calcareous sediments and sedimentary rocks by loss on ignition: Comparison with other methods. *SEPM Journal of Sedimentary Research*, *44*, 242–248. https://doi.org/10.1306/74D729D2-2B21-11D7-8648000102C1865D

Dearing, J. (1999). *Environmental magnetic susceptibility: Using the Bartington MS2 System*, (2nd ed.). Kenilworth, England: Chi Publishing.

Dubois, N., Kienast, M., Kienast, S., Normandeau, C., Calvert, S. E., Herbert, T. D., & Mix, A. (2011). Millennial-scale variations in hydrography and biogeochemistry in the Eastern Equatorial Pacific over the last 100 kyr. *Quaternary Science Reviews*, *30*, 210–223. https://doi.org/10.1016/j.quascirev.2010.10.012

Faegri, K., Kaland, P. E., & Krzywinski, K. (1989). *Textbook of pollen analysis*, (4th ed.). Chichester [England] ; New York: Wiley.

Glover, K. C., MacDonald, G. M., Kirby, M. E., Rhodes, E. J., Stevens, L., Silveira, E., & Whitaker, A. (2017). Evidence for orbital and North Atlantic climate forcing in alpine Southern California between 125 and 10 ka from multi-proxy analyses of Baldwin Lake. *Quaternary Science Reviews*, *167*, 47–62. https://doi.org/10.1016/j.quascirev.2017.04.028

Grimm, E. C. (1987). CONISS: A FORTRAN 77 program for stratigraphically constrained cluster analysis by the method of incremental sum of squares. *Computational Geosciences*, *13*, 13–35. https://doi.org/10.1016/0098-3004(87)90022-7

Herbert, T. D., Schuffert, J. D., Andreasen, D., Heusser, L. E., Lyle, M., Mix, A., et al. (2001). Collapse of the California current during glacial maxima linked to climate change on land. *Science*, *293*(5527), 71–76. https://doi.org/10.1126/science.1059209

Herring, E. M., & Gavin, D. G. (2015). Climate and vegetation since the Last Interglacial (MIS 5e) in a putative glacial refugium, northern Idaho, USA. *Quaternary Science Reviews*, *117*, 82–95. https://doi.org/10.1016/j.quascirev.2015.03.028

Heusser, L. E. (2000). Rapid oscillations in western North America vegetation and climate during oxygen isotope stage 5 inferred from pollen data from Santa Barbara Basin (Hole 893A). *Palaeogeography Palaeoclimatology Palaeoecology*, *161*, 407–421. https://doi.org/10.1016/S0031-0182(00)00096-1

Heusser, L. E., Kirby, M. E., & Nichols, J. E. (2015). Pollen-based evidence of extreme drought during the last Glacial (32.6–9.0 ka) in coastal southern California. *Quaternary Science Reviews*, *126*, 242–253. https://doi.org/10.1016/j.quascirev.2015.08.029

Heusser, L. E., & Sirocko, F. (1997). Millennial pulsing of environmental change in southern California from the past 24 k.y.: A record of Indo-Pacific ENSO events? *Geology*, *25*, 243. https://doi.org/10.1130/0091-7613(1997)025<0243:MPOECI>2.3.CO;2

IPCC (2013). *Climate Change 2013: The Physical Science Basis. Contribution of Working Group I to the Fifth Assessment Report of the Intergovernmental Panel on Climate Change*. Cambridge, United Kingdom and New York, NY, USA: Cambridge University Press.

Jiménez-Moreno, G., Anderson, R. S., Desprat, S., Grigg, L. D., Grimm, E. C., Heusser, L. E., et al. (2010). Millennial-scale variability during the last glacial in vegetation records from North America. *Quaternary Science Reviews*, *29*, 2865–2881. https://doi.org/10.1016/j.quascirev.2009.12.013

Keeley, J. E., Bond, W. J., Bradstock, R. A., Pausas, J., & Rundel, P. W. (2012). *Fire in Mediterranean ecosystems: Ecology, evolution and management*. Cambridge, UK; New York: Cambridge University Press.

Kelly, A. E., & Goulden, M. L. (2008). Rapid shifts in plant distribution with recent climate change. *Proceedings of the National Academy of Sciences*, *105*(33), 11823–11826. https://doi.org/10.1073/pnas.0802891105

Kirby, M. E., Heusser, L., Scholz, C., Ramezan, R., Anderson, M. A., Markle, B., et al. (2018). A late Wisconsin (32-10k cal a BP) history of pluvials, droughts and vegetation in the Pacific south-west United States (Lake Elsinore, CA). *Journal of Quaternary Science*, *33*, 238–254. https://doi.org/10.1002/jqs.3018

Kirby, M. E., Lund, S. P., & Bird, B. W. (2006). Mid-Wisconsin sediment record from Baldwin Lake reveals hemispheric climate dynamics (Southern CA, USA). *Palaeogeography Palaeoclimatology Palaeoecology*, *241*, 267–283. https://doi.org/10.1016/j.palaeo.2006.03.043

Kirby, M. E., Zimmerman, S. R. H., Patterson, W. P., & Rivera, J. J. (2012). A 9170-year record of decadal-to-multi-centennial scale pluvial episodes from the coastal Southwest United States: A role for atmospheric rivers? *Quaternary Science Reviews*, *46*, 57–65. https://doi.org/10.1016/j.quascirev.2012.05.008

Kylander, M. E., Ampel, L., Wohlfarth, B., & Veres, D. (2011). High-resolution X-ray fluorescence core scanning analysis of Les Echets (France) sedimentary sequence: new insights from chemical proxies. *Journal of Quaternary Science*, *26*, 109–117. https://doi.org/10.1002/jqs.1438

Laskar, J., Robutel, P., Joutel, F., Gastineau, M., Correia, A. C. M., & Levrard, B. (2004). A long-term numerical solution for the insolation quantities of the Earth. *Astronomy and Astrophysics*, *428*, 261–285. https://doi.org/10.1051/0004-6361:20041335

Lenihan, J. M., Bachelet, D., Neilson, R. P., & Drapek, R. (2008). Response of vegetation distribution, ecosystem productivity, and fire to climate change scenarios for California. *Climatic Change*, *87*, 215–230.

Lisiecki, L. E., & Raymo, M. E. (2005). A Pliocene-Pleistocene stack of 57 globally distributed benthic δ 18 O records: PLIOCENE-PLEISTOCENE BENTHIC STACK. *Paleoceanography*, *20*, –PA1003. https://doi.org/10.1029/2004PA001071

Loisel, J., MacDonald, G. M., & Thomson, M. J. (2017). Little Ice Age climatic erraticism as an analogue for future enhanced hydroclimatic variability across the American Southwest. *PLoS ONE*, *12*(10), e0186282. https://doi.org/10.1371/journal.pone.0186282

Lyle, M., Heusser, L., Ravelo, C., Andreasen, D., Olivarez Lyle, A., & Diffenbaugh, N. (2010). Pleistocene water cycle and eastern boundary current processes along the California continental margin. *Paleoceanography*, *25*, PA4211. https://doi.org/10.1029/2009PA001836

Meyers, P. A. (1994). Preservation of elemental and isotopic source identification of sedimentary organic matter. *Chemical Geology*, *114*, 289–302.

Minnich, R. A. (1976). Vegetation of the San Bernardino Mountains. In *Symposium Proceedings: Plant Communities of Southern California; 1974 May 4; Fullerton, CA*, (pp. 99–124). Berkeley, CA: California Native Plant Society.

Minnich, R. A. (1984). Snow drifting and timberline dynamics on Mount San Gorgonio, California, USA. *Arctic and Alpine Research*, *16*, 395. https://doi.org/10.2307/1550901

Minnich, R. A., Barbour, M. G., Burk, J. H., & Fernau, R. F. (1995). Sixty years of change in Californian Conifer Forests of the San Bernardino Mountains. *Conservation Biology*, *9*, 902–914. https://doi.org/10.1046/j.1523-1739.1995.09040902.x

Minyuk, P. S., Brigham-Grette, J., Melles, M., Borkhodoev, V. Y., & Glushkova, O. Y. (2006). Inorganic geochemistry of El'gygytgyn Lake sediments (northeastern Russia) as an indicator of paleoclimatic change for the last 250 kyr. *Journal of Paleolimnology*, *37*(1), 123–133. https://doi.org/10.1007/s10933-006-9027-4

Myrbo, A., Lynch, B., Curran, S., 2005. Limnological Research Center Core Facility SOP Series charcoal-sieve.pdf.

NOAA, 2019. What are "proxy" data? [WWW Document]. Natl. Cent. Environ. Inf. URL https://www.ncdc.noaa.gov/news/what-are-proxy-data

Olson, D. M., Dinerstein, E., Wikramanayake, E. D., Burgess, N. D., Powell, G. V. N., Underwood, E. C., et al. (2001). Terrestrial ecoregions of the world: A new map of life on Earth. *Bioscience*, *51*, 933. https://doi.org/10.1641/0006-3568(2001)051[0933:TEOTWA]2.0.CO;2

Oster, J. L., Ibarra, D. E., Winnick, M. J., & Maher, K. (2015). Steering of westerly storms over western North America at the Last Glacial Maximum. *Nature Geoscience*, *8*(3), 201–205. https://doi.org/10.1038/ngeo2365

Overpeck, J., Garfin, G., Jardine, A., Busch, D. E., Cayan, D., Dettinger, M., et al. (2013). Summary for Decision Makers. In G. Garfin, A. Jardine, R. Merideth, M. Black, & S. LeRoy (Eds.), *Assessment of climate change in the Southwest United States*, (pp. 1–20). Washington, DC: Island Press/Center for Resource Economics.

Owen, L. A., Clemmens, S. J., Finkel, R. C., & Gray, H. (2014). Late Quaternary alluvial fans at the eastern end of the San Bernardino Mountains, Southern California. *Quaternary Science Reviews*, *87*, 114–134. https://doi.org/10.1016/j.quascirev.2014.01.003

Pickarski, N., Kwiecien, O., Djamali, M., & Litt, T. (2015). Vegetation and environmental changes during the last interglacial in eastern Anatolia (Turkey): a new high-resolution pollen record from Lake Van. *Palaeogeography Palaeoclimatology Palaeoecology*, *435*, 145–158. https://doi.org/10.1016/j.palaeo.2015.06.015

Seager, R., Osborn, T. J., Kushnir, Y., Simpson, I. R., Nakamura, J., & Liu, H. (2019). Climate variability and change of Mediterranean-type climates. *Journal of Climate*, *32*(10), 2887–2915. https://doi.org/10.1175/JCLI-D-18-0472.1

Stevens, J. T., Safford, H. D., Harrison, S., & Latimer, A. M. (2015). Forest disturbance accelerates thermophilization of understory plant communities. *Journal of Ecology*, *103*, 1253–1263. https://doi.org/10.1111/1365-2745.12426

Stevens, M., Corina, K., 2016. 26 million trees have died in the Sierra since October, raising fire risk. Los Angel. Times.

Swain, D. L., Langenbrunner, B., Neelin, J. D., & Hall, A. (2018). Increasing precipitation volatility in twenty-first-century California. *Nature Climate Change*, *8*, 427–433. https://doi.org/10.1038/s41558-018-0140-y

Thevenon, F., Adatte, T., Spangenberg, J. E., & Anselmetti, F. S. (2012). Elemental (C/N ratios) and isotopic ($\delta^{15}N_{org}$, $\delta^{13}C_{org}$) compositions of sedimentary organic matter from a high-altitude mountain lake (Meidsee, 2661 m a.s.l., Switzerland): Implications for Lateglacial and Holocene Alpine landscape evolution. *The Holocene*, *22*, 1135–1142. https://doi.org/10.1177/0959683612441841

Thompson, R., & Oldfield, F. (1986). *Environmental magnetism*. London: Allen & Unwin (Publishers) Ltd.

Tubbs, A. M. (1972). Summer thunderstorms over Southern California. *Monthly Weather Review*, *100*, 799–807. https://doi.org/10.1175/1520-0493(1972)100<0799:STOSC>2.3.CO;2

Tullis, P. (2013). *Into the Wildfire*. N. Y: Times Mag.

Tzedakis, P. C. (2005). Towards an understanding of the response of southern European vegetation to orbital and suborbital climate variability. *Quaternary Science Reviews*, *24*, 1585–1599. https://doi.org/10.1016/j.quascirev.2004.11.012

U.S. Climate Data [WWW Document], 2016. US Clim. Data Big Bear Lake - Calif. URL http://www.usclimatedata.com/climate/big-bear-lake/california/united-states/usca0094 (accessed 8.8.16).

Underwood, E. C., Viers, J. H., Klausmeyer, K. R., Cox, R. L., & Shaw, M. R. (2009). Threats and biodiversity in the mediterranean biome. *Diversity and Distributions*, *15*, 188–197. https://doi.org/10.1111/j.1472-4642.2008.00518.x

USDA Forest Service, 2005. Part 1 Southern California National Forests Vision (No. R5- MB- 075), USDA Land Management Plan. United States Department of Agriculture Forest Service - Pacific Southwest Region.

van Mantgem, P. J., Stephenson, N. L., Byrne, J. C., Daniels, L. D., Franklin, J. F., Fule, P. Z., et al. (2009). Widespread increase of tree mortality rates in the Western United States. *Science*, *323*(5913), 521–524. https://doi.org/10.1126/science.1165000

Westerling, A. L. (2006). Warming and earlier spring increase Western U.S. forest wildfire activity. *Science*, *313*(5789), 940–943. https://doi.org/10.1126/science.1128834

Whitlock, C., & Grigg, L. D. (1999). Paleoecological evidence of Milankovitch and Sub-Milankovitch climate variations in the western U.S. during the late quaternary. In U. Clark, S. Webb, & D. Keigwin (Eds.), *Geophysical Monograph Series*, (pp. 227–241). Washington, D. C.: American Geophysical Union. https://doi.org/10.1029/GM112p0227

Woolfenden, W. B. (2003). A 180,000-year pollen record from Owens Lake, CA: terrestrial vegetation change on orbital scales. *Quaternary Research*, *59*, 430–444. https://doi.org/10.1016/S0033-5894(03)00033-4

References From the Supporting Information

Adam, D. P., Sims, J. D., & Throckmorton, C. K. (1981). 130,000-yr continuous pollen record from Clear Lake, Lake County, California. *Geology*, *9*, 373. https://doi.org/10.1130/0091-7613(1981)9<373:YCPRFC>2.0.CO;2

Adam, D. P., & West, G. J. (1983). Temperature and precipitation estimates through the last glacial cycle from Clear Lake, California, Pollen Data. *Science*, *219*(4581), 168–170. https://doi.org/10.1126/science.219.4581.168

Anderson, R. S., Starratt, S., Jass, R. M. B., & Pinter, N. (2010). Fire and vegetation history on Santa Rosa Island, Channel Islands, and long-term environmental change in southern California. *Journal of Quaternary Science*, *25*, 782–797. https://doi.org/10.1002/jqs.1358

Benson, L. V., Kashgarian, M., Rye, R. O., Lund, S. P., Paillet, F., Smoot, J. P., et al. (2002). Holocene multidecadal and multicentennial droughts affecting northern California and Nevada. *Quaternary Science Reviews*, *21*, 659–682.

Bird, B. W., & Kirby, M. E. (2006). An alpine lacustrine record of Early Holocene North American monsoon dynamics from Dry Lake, Southern California (USA). *Journal of Paleolimnology*, *35*(1), 179–192. https://doi.org/10.1007/s10933-005-8514-3

Bird, B. W., Kirby, M. E., Howat, I. M., & Tulaczyk, S. (2010). Geophysical evidence for Holocene lake-level change in southern California (Dry Lake). *Boreas*, *39*, 131–144. https://doi.org/10.1111/j.1502-3885.2009.00114.x

Blaauw, M. (2012). Out of tune: The dangers of aligning proxy archives. *Quaternary Science Reviews*, *36*, 38–49. https://doi.org/10.1016/j.quascirev.2010.11.012

Briles, C. E., Whitlock, C., & Bartlein, P. J. (2005). Postglacial vegetation, fire, and climate history of the Siskiyou Mountains, Oregon, USA. *Quaternary Research*, *64*, 44–56. https://doi.org/10.1016/j.yqres.2005.03.001

Briles, C. E., Whitlock, C., Bartlein, P. J., & Higuera, P. (2008). Regional and local controls on postglacial vegetation and fire in the Siskiyou Mountains, northern California, USA. *Palaeogeography Palaeoclimatology Palaeoecology*, *265*, 159–169. https://doi.org/10.1016/j.palaeo.2008.05.007

Briles, C. E., Whitlock, C., Skinner, C. N., & Mohr, J. (2011). Holocene forest development and maintenance on different substrates in the Klamath Mountains, northern California, USA. *Ecology*, *92*, 590–601. https://doi.org/10.1890/09-1772.1

Brunelle, A., & Anderson, R. S. (2003). Sedimentary charcoal as an indicator of late-Holocene drought in the Sierra Nevada, California, and its relevance to the future. *The Holocene*, *13*, 21–28. https://doi.org/10.1191/0959683603hl591rp

Cole, K. L., & Liu, G.-W. (1994). Holocene paleoecology of an estuary on Santa Rosa Island, California. *Quaternary Research*, *41*, 326–335. https://doi.org/10.1006/qres.1994.1037

Daniels, M. L., Anderson, R. S., & Whitlock, C. (2005). Vegetation and fire history since the Late Pleistocene from the Trinity Mountains, northwestern California, USA. *The Holocene*, *15*, 1062–1071. https://doi.org/10.1191/0959683605hl878ra

Davis, O. K. (1992). Rapid climatic change in coastal southern California inferred from pollen analysis of San Joaquin Marsh. *Quaternary Research*, *37*, 89–100. https://doi.org/10.1016/0033-5894(92)90008-7

Davis, O. K. (1999b). Pollen analysis of a late-glacial and Holocene sediment core from Mono Lake, Mono County, California. *Quaternary Research*, *52*, 243–249.

Davis, O. K., & Moratto, M. J. (1988). Evidence for a warm dry early Holocene in the western Sierra Nevada of California: Pollen and plant macrofossil analysis of Dinkey and Exchequer Meadows. *Madroño*, *35*, 132–149.

Davis, O. K., Scott Anderson, R., Fall, P. L., O'Rourke, M. K., & Thompson, R. S. (1985). Palynological evidence for early Holocene aridity in the southern Sierra Nevada, California. *Quaternary Research*, *24*, 322–332. https://doi.org/10.1016/0033-5894(85)90054-7

Grigg, L. D., & Whitlock, C. (1998). Late-glacial vegetation and climate change in western Oregon. *Quaternary Research*, *49*, 287–298.

Grigg, L. D., & Whitlock, C. (2002). Patterns and causes of millennial-scale climate change in the Pacific Northwest during Marine Isotope Stages 2 and 3. *Quaternary Science Reviews*, *21*, 2067–2083. https://doi.org/10.1016/S0277-3791(02)00017-3

Grigg, L. D., & Whitlock, C. L. (2001). Evidence for millennial-scale climate change during Marine Isotope Stages 2 and 3 at Little Lake, Western Oregon, U.S.A. *Quaternary Research*, *56*, 10–22.

Hakala, K. J., & Adam, D. P. (2004). Late Pleistocene vegetation and climate in the southern cascade range and the Modoc Plateau Region. *Journal of Paleolimnology*, *31*, 189–215. https://doi.org/10.1023/B:JOPL.0000019231.58234.fb

Heusser, L.E., 1995. Pollen stratigraphy and paleoecologic interpretation of the 160-ky record from Santa Barbara Basin, Hole 893A1, in: In Proceedings of the Ocean Drilling Program, Scientific Results. pp. 265–279.

Koehler, P. A., & Anderson, R. S. (1994). The paleoecology and stratigraphy of Nichols Meadow, Sierra National Forest, California, USA. *Palaeogeography Palaeoclimatology Palaeoecology*, *112*, 1–17. https://doi.org/10.1016/0031-0182(94)90132-5

Litwin, R.J., Adam, D.P., Frederiksen, N.O., Woolfenden, W.B., 1997. An 800,000-year pollen record from Owens Lake, California; preliminary analyses, in: Special Paper 317: An 800,000-Year Paleoclimatic Record from Core OL-92, Owens Lake, Southeast California. Geological Society of America, pp. 127–142.

Litwin, R. J., Smoot, J. P., Durika, N. J., & Smith, G. I. (1999). Calibrating Late Quaternary terrestrial climate signals: Radiometrically dated pollen evidence. *Quaternary Science Reviews*, *18*, 1151–1171.

Long, C. J., & Whitlock, C. (2002). Fire and vegetation history from the coastal rain forest of the Western Oregon Coast Range. *Quaternary Research*, *58*, 215–225. https://doi.org/10.1006/qres.2002.2378

Mahan, S. A., Gray, H. J., Pigati, J. S., Wilson, J., Lifton, N. A., Paces, J. B., & Blaauw, M. (2014). A geochronologic framework for the Ziegler Reservoir fossil site, Snowmass Village, Colorado. *Quaternary Research*, *82*, 490–503. https://doi.org/10.1016/j.yqres.2014.03.004

Mensing, S. A., Benson, L. V., Kashgarian, M., & Lund, S. (2004). A Holocene pollen record of persistent droughts from Pyramid Lake, Nevada, USA. *Quaternary Research*, *62*, 29–38. https://doi.org/10.1016/j.yqres.2004.04.002

Mohr, J. A., Whitlock, C., & Skinner, C. N. (2000). Postglacial vegetation and fire history, eastern Klamath Mountains, California, USA. *The Holocene*, *10*, 587–601. https://doi.org/10.1191/095968300675837671

Sea, D. S., & Whitlock, C. (1995). Postglacial vegetation and climate of the Cascade Range, Central Oregon. *Quaternary Research*, *43*, 370–381. https://doi.org/10.1006/qres.1995.1043

Smith, S. J., & Anderson, R. S. (1992). Late Wisconsin paleoecologic record from Swamp Lake, Yosemite National Park, California. *Quaternary Research*, *38*, 91–102. https://doi.org/10.1016/0033-5894(92)90032-E

Street, J. H., Anderson, R. S., & Paytan, A. (2012). An organic geochemical record of Sierra Nevada climate since the LGM from Swamp Lake, Yosemite. *Quaternary Science Reviews*, *40*, 89–106. https://doi.org/10.1016/j.quascirev.2012.02.017

Walsh, M. K., Whitlock, C., & Bartlein, P. J. (2008). A 14,300-year-long record of fire–vegetation–climate linkages at Battle Ground Lake, southwestern Washington. *Quaternary Research*, *70*, 251–264.

Whitlock, C., Sarna-Wojcicki, A. M., Bartlein, P. J., & Nickmann, R. J. (2000). Environmental history and tephrostratigraphy at Carp Lake, southwestern Columbia Basin, Washington, USA. *Palaeogeography Palaeoclimatology Palaeoecology*, *155*, 7–29. https://doi.org/10.1016/S0031-0182(99)00092-9

Worona, M. A., & Whitlock, C. L. (1995). Late Quaternary vegetation and climate history near Little Lake, central Coast Range, Oregon. *GSA Bulletin*, *107*, 867–876.